Supplementary Information

In Vivo Mitochondrial Base Editing Restores Genotype and Visual Function in a Mouse Model of LHON

Supplementary Figures

Supplementary Tables

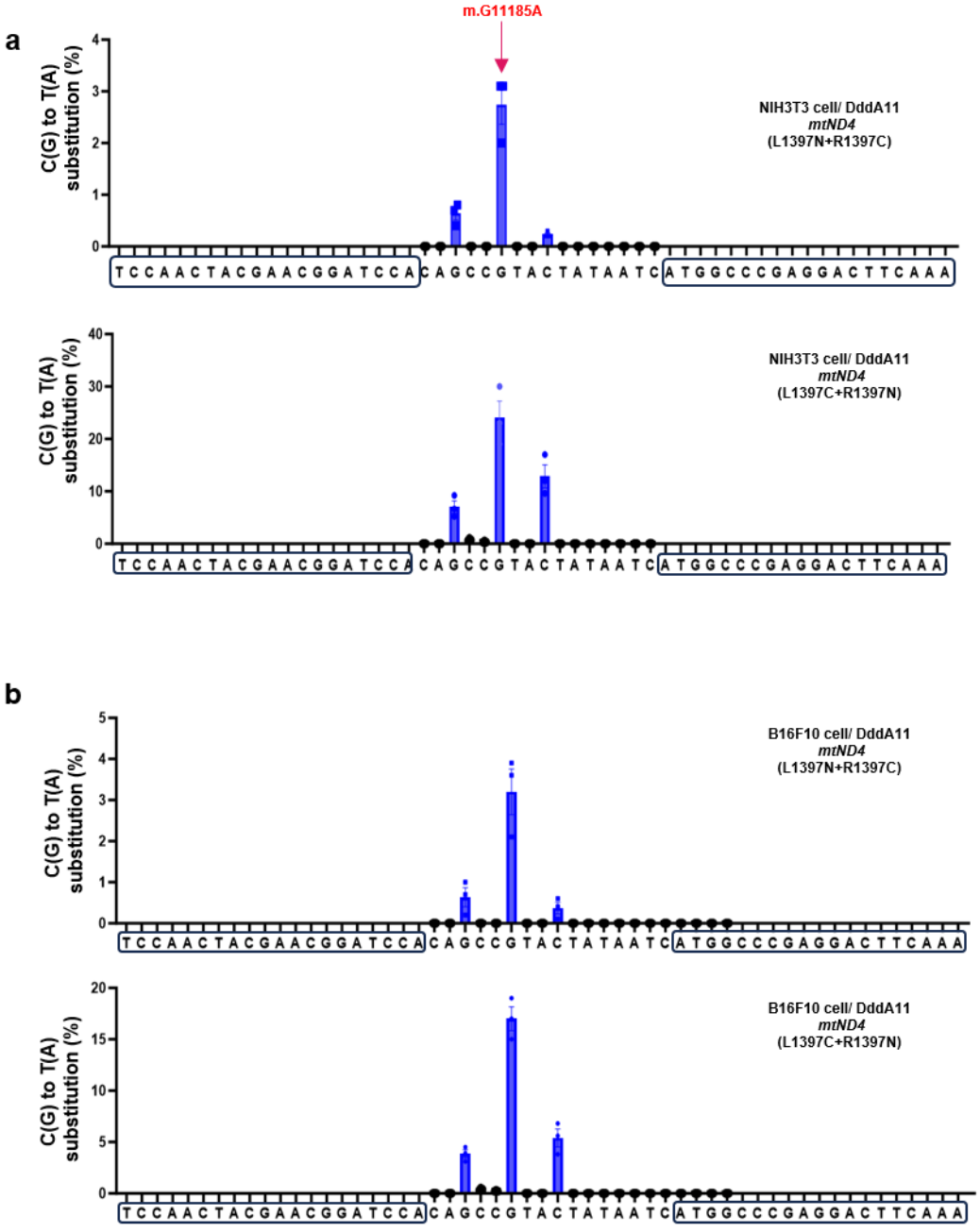

Supplementary Figure 1

Supplementary Figure 1. DddA11 deaminase-mediated C(G) to T(A) base editing on mouse *MT-ND4* gene target locus.

a. Targeted C(G) to T(A) base editing on mouse *MT-ND4* gene in DddA11 transfected NIH3T3 cells. TALE sequence shown in navy box and desired locus shown in red arrow (m.G11185A). Each TALE combinations were indicated in the right upper of graphs. Error bars indicate standard error of the mean (s.e.m.) for biologically independent sample.

b. Targeted C(G) to T(A) base editing on mouse *MT-ND4* gene in DddA11 transfected B16F10 cells. TALE sequence shown in navy box and desired locus shown in red arrow (m.G11185A). Each TALE combinations were indicated in the right upper of graphs. Error bars indicate standard error of the mean (s.e.m.) for biologically independent sample.

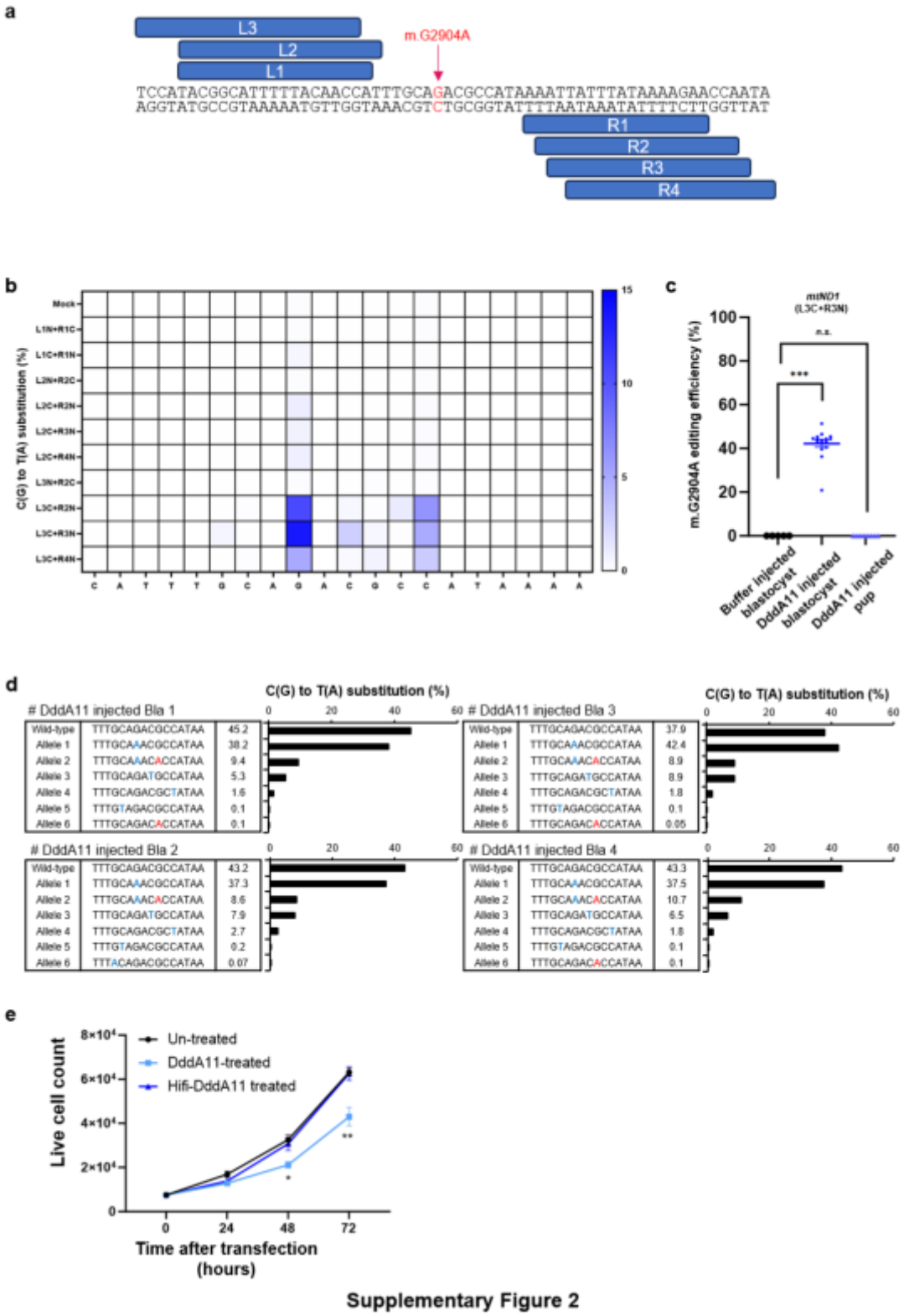

Supplementary Figure 2

Supplementary Figure 2. Generation of DddA11 for inducing m.G2904A base editing on *MT-ND1* gene, and its limitations for manufacturing *MT-ND1* mutant mice.

a. TALE combinations for m.G2904 targeted DddA11.

b. Heatmap indicating C(G) to T(A) editing efficiency at targeted *MT-ND1* gene loci induced by each TALE combined DddA11. Error bars indicate standard error of the mean (s.e.m.) for biologically independent sample.

c. Editing efficiency of m.G2904A buffer injected blastocysts (n=5), DddA11 injected blastocysts (n=16) and DddA11 injected pups (n=8). Error bars indicate standard error of the mean (s.e.m.) for biologically independent sample. The exact p-values were 7.90293E-14 in buffer injected blastocysts and DddA11 injected blastocysts, 0.06 in buffer injected blastocysts and DddA11 injected pups. (*n.s.*, not significant, ***p<0.001 using Student's two-tailed t-test).

d. *MT-ND1* gene mutation alleles induced by DddA11 in blastocysts. Desired editing locus was shown in red (m.G2904A), and undesired editing loci were in blue.

e. Comparison of live cell counts in B16F10 cells with DddA11 and Hifi-DdCBE transfected after 72 hours. Error bars indicate standard error of the mean (s.e.m.) for biologically independent sample (n=3). (*p<0.05, ** p<0.01 using Student's two-tailed t-test).

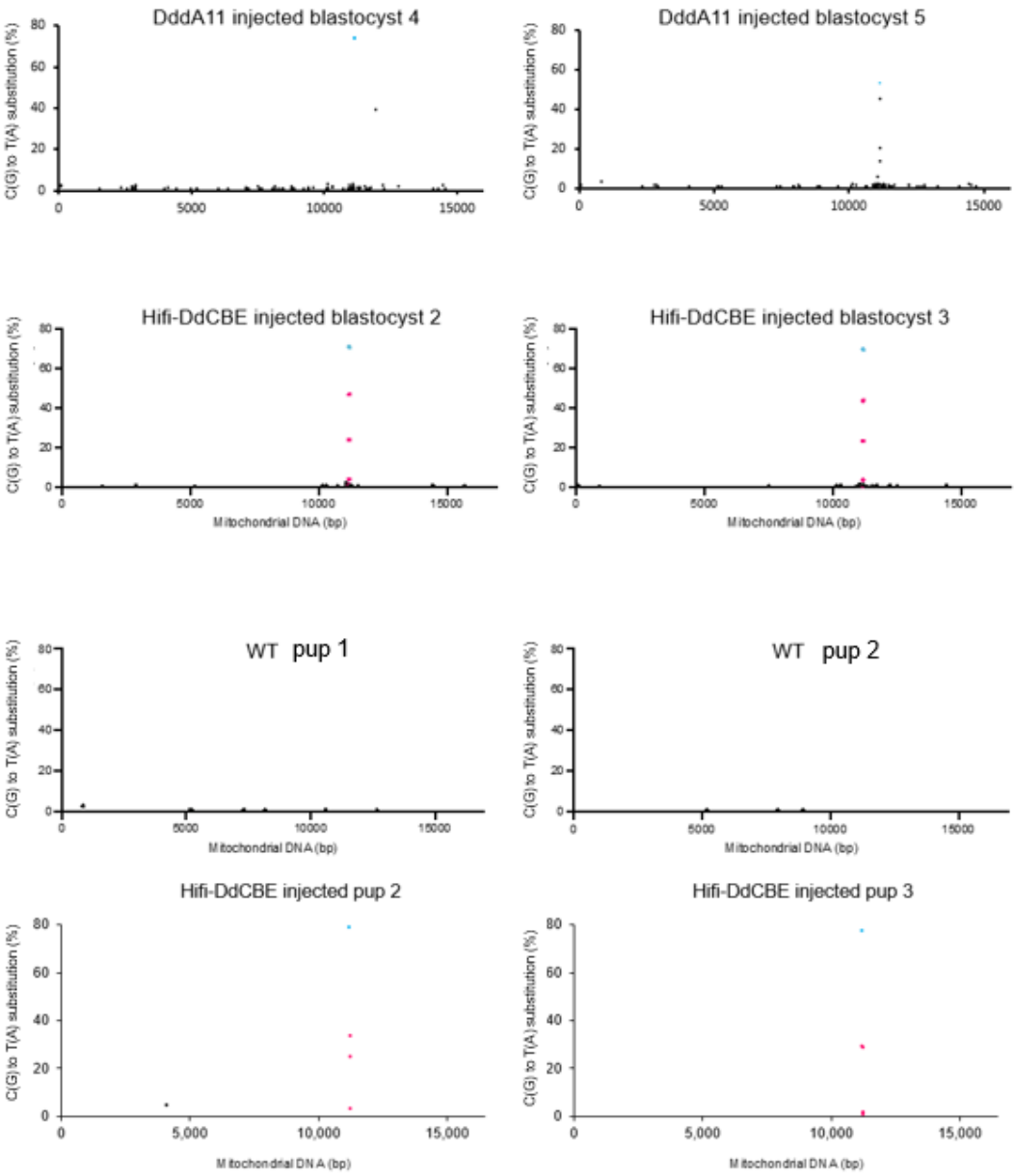

Supplementary Figure 3

Supplementary Figure 3. Base substitution of DddA11 and Hifi-DdCBE mediated whole mitochondrial genome in blastocyst and pup.

C(G) to T(A) base substitution in whole mitochondrial genome of DddA11 injected, Hifi-DdCBE injected blastocysts, WT pups and Hifi-DdCBE injected pups. Each dot represents C(G) to T(A) substitution on whole mitochondrial genome. On-target editing efficiencies were colored with cyan, and the undesired editing efficiencies were colored pink.

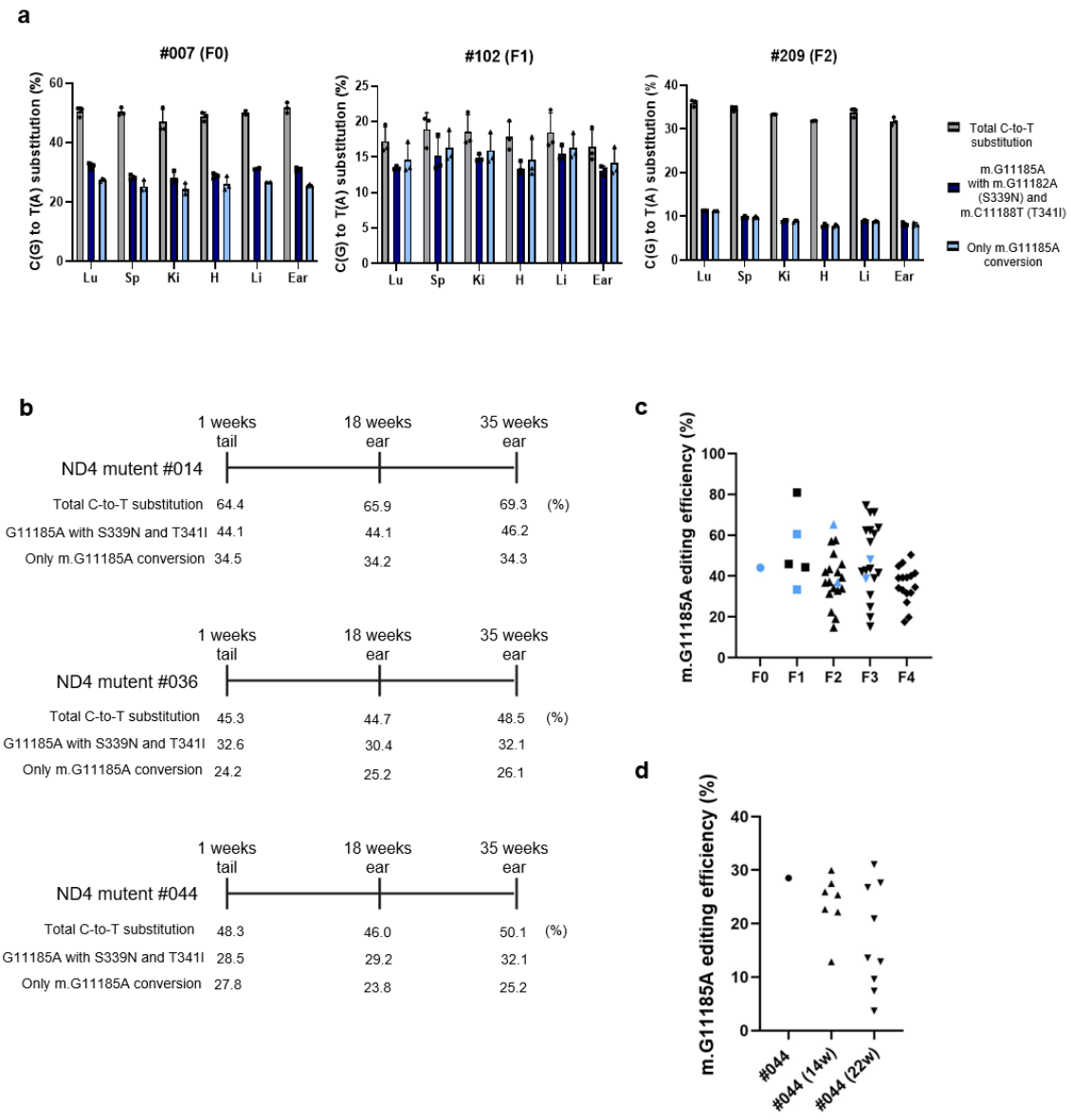

Supplementary Figure 4

Supplementary Figure 4. Different tissue, time-course, and germline transmission analysis editing efficiencies in *MT-ND4* mutant mice.

a. Editing efficiency of various tissues from F0, F1, and F2 mice. Genomic DNA was extracted from tissues at least 6 weeks post-birth. Gray, navy, and skyblue bars represent the frequencies of total C(G) to T(A), m.G11185A with m.G11182A and m.C11188T, and only m.G11185A conversions, respectively. Error bars represent the standard error of the mean (s.e.m.) for three replicates (n=3). (Lu: lung, Sp: spleen, Ki: Kidney, H: heart, Li: liver).

b. Timeline of genomic DNA collection and editing efficiencies in three *MT-ND4* mutant mice over time (1 week from tail, 18 weeks and 35 weeks from ear). Percentages represent total C-to-T conversion, m.G11185A with m.G11182A and m.C11188T, and only m.G11185A conversion at each timeline.

c. m.G11185A mutation loads of mutant mice in F0-F4 mutant mice. Blue colored shapes indicate mother mutant mice of each generation.

d. Editing efficiency at m.G11185A locus of F0 and F1 mice with different time point of childbirth of F0 #044.

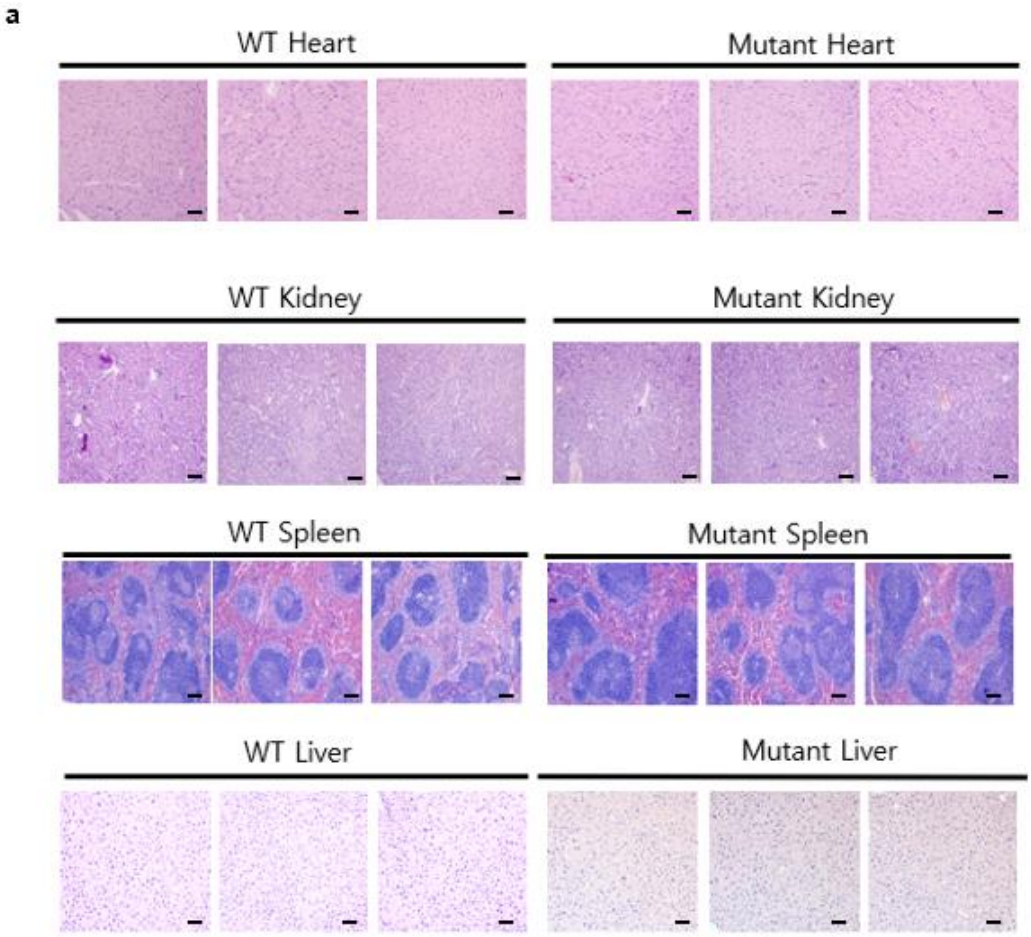

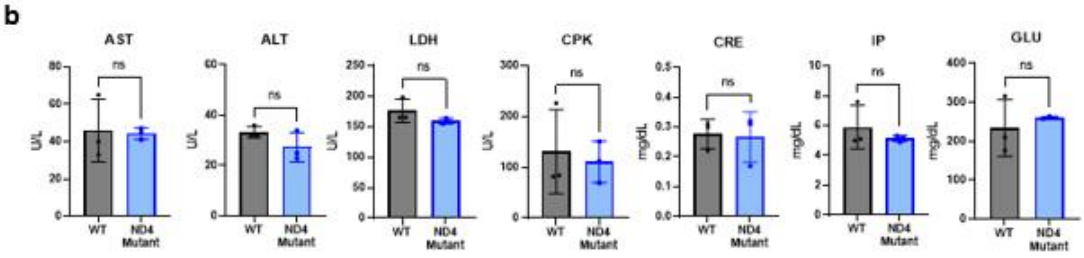

Supplementary Figure 5

Supplementary Figure 5. Histological and serum analysis of WT and *MT-ND4* mutant mice.

a. H&E staining results of WT and *ND4* mutant mice. Each slides were tissues from biologically independent mice. (scale bar: 20 μm).

b. Serum analysis of WT and *ND4* mutant mice.
(AST : Aspartate Aminotransferase, ALT: Alanine Aminotransferase, LDH : Lactate Dehydrogenase CPK : Creatine Phosphokinase, CRE : Creatinine, IP : Inorganic Phosphate, GLU : Glucose)
Error bars represent the standard error of the mean (s.e.m.) for biologically independent mice (n=3) (ns, not significant using Student's two-tailed t-test).

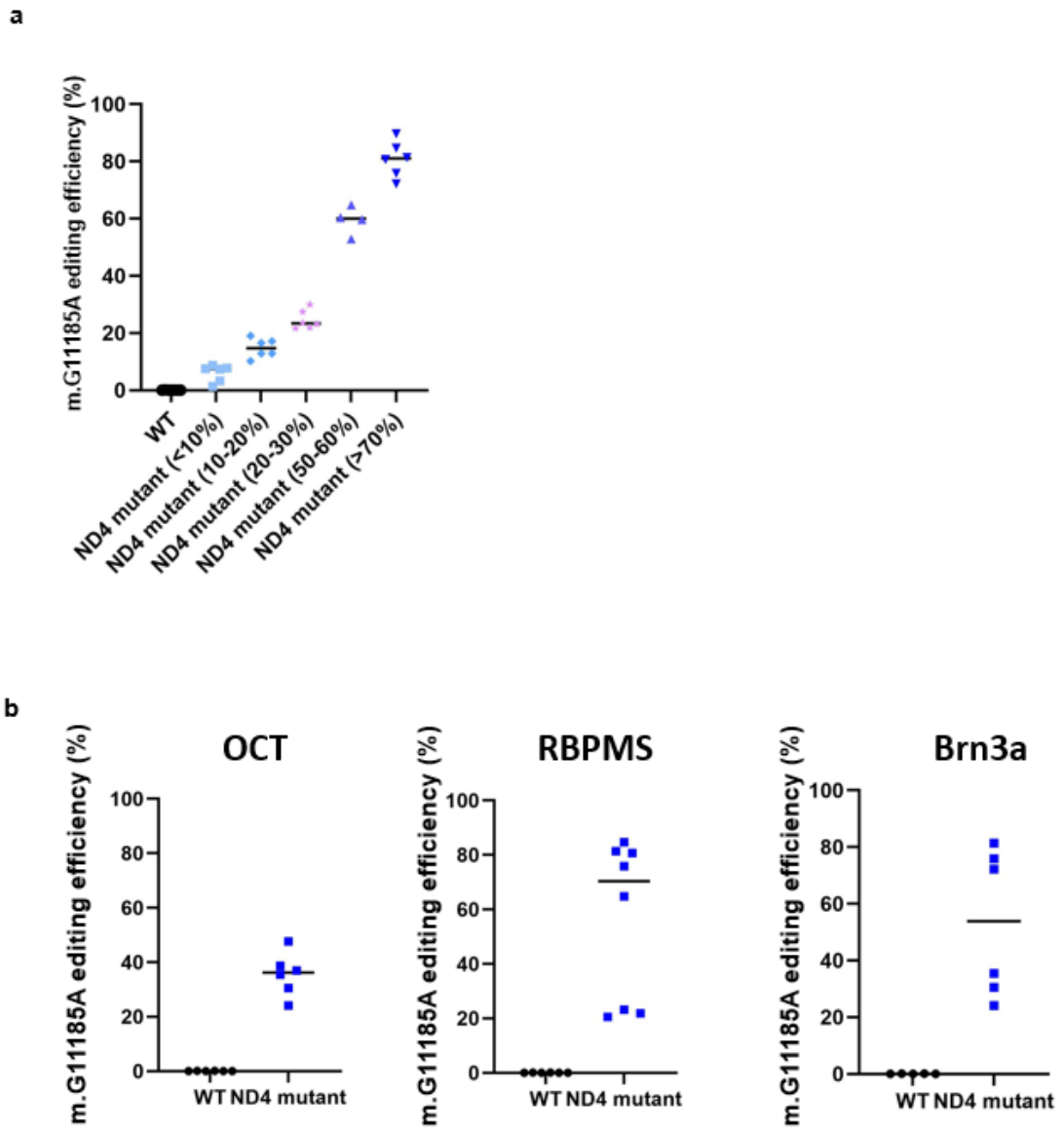

Supplementary Figure 6

Supplementary Figure 6. Genotyping results of *ND4* mutant mice used in histological analysis.

a. Genotyping results of *ND4* mutant related to Fig. 3a-d. Each dot blots mean individual mutant mice. Each dot blot indicates individual mice.

b. Genotyping results of *ND4* mutant related to Fig. 3e (OCT), 3i (RBPMS IHC), 3k (Brn3a IF). Each dot blot indicates individual mice. Bars indicate median value.

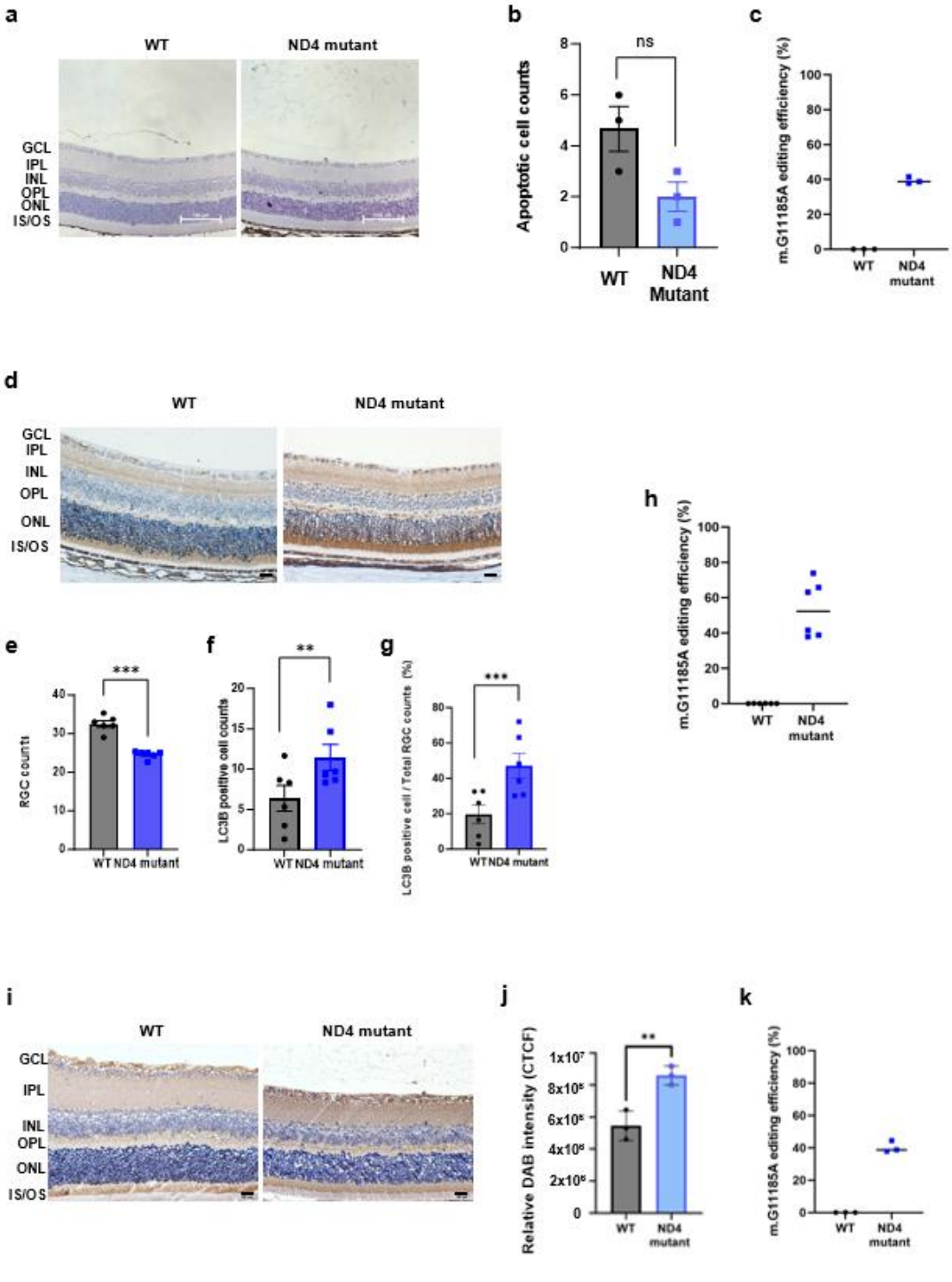

Supplementary Figure 7

Supplementary Figure 7. Immunohistochemical analysis of retina on *MT-ND4* mutant mice.

a. Immunohistochemical staining for Cleaved Caspase-3 in WT, and *MT-ND4* mutant mice. (scale bar: 100 μm)

b. Quantification of apoptotic cells in GCL between WT and *MT-ND4* mutant mice. The exact p-values for *MT-ND4* mutant mice compared with WT mice was 0.064. Error bars indicate s.e.m. for biologically independent mice (n=3) (ns, not significant using Student's two-tailed t-test).

c. Genotyping results for *ND4* mutant mice used in caspase-3 IHC. Bar indicate median value.

d. Immunohistochemical staining for autophagy markers (LC3B) in WT and *MT-ND4* mutant mice. (scale bar: 20 μm).

e. Quantification of RGCs between WT and *MT-ND4* mutant mice. The exact p-values for *MT-ND4* mutant mice compared with WT mice was 0.0006. Error bars indicate s.e.m. for biologically independent mice (n=6) (*** p<0.001 using Student's two-tailed t-test).

f. Quantification of LC3B-positive RGCs between WT and *MT-ND4* mutant mice. The exact p-values for *MT-ND4* mutant mice compared with WT mice was 0.0025. Error bars indicate s.e.m. for biologically independent mice (n=6) (** p<0.01 using Student's two-tailed t-test).

g. Quantification of autophagy-positive ratio of RGCs between WT and *MT-ND4* mutant mice. The exact p-values for *MT-ND4* mutant mice compared with WT mice was <0.0001. Error bars indicate s.e.m. for biologically independent mice (n=6) (*** p<0.001 using Student's two-tailed t-test).

h. Genotyping results for *MT-ND4* mutant mice used in LC3B IHC. Bar indicate median value.

i. Immunohistochemical staining for neuroinflammation markers, glial fibrillary acidic protein (GFAP) in WT and *MT-ND4* mutant mice. (scale bar: 20 μm).

j. Quantification of neuro-inflammation positive areas in retina of WT and *MT-ND4* mutant mice. The exact p-values for *MT-ND4* mutant mice compared with WT mice was 0.008. Error bars indicate s.e.m. for biologically independent mice (n=3) (** $p<0.01$ using Student's two-tailed t-test).

k. Genotyping results for *MT-ND4* mutant mice used in GFAP IHC. Bar indicate median value.

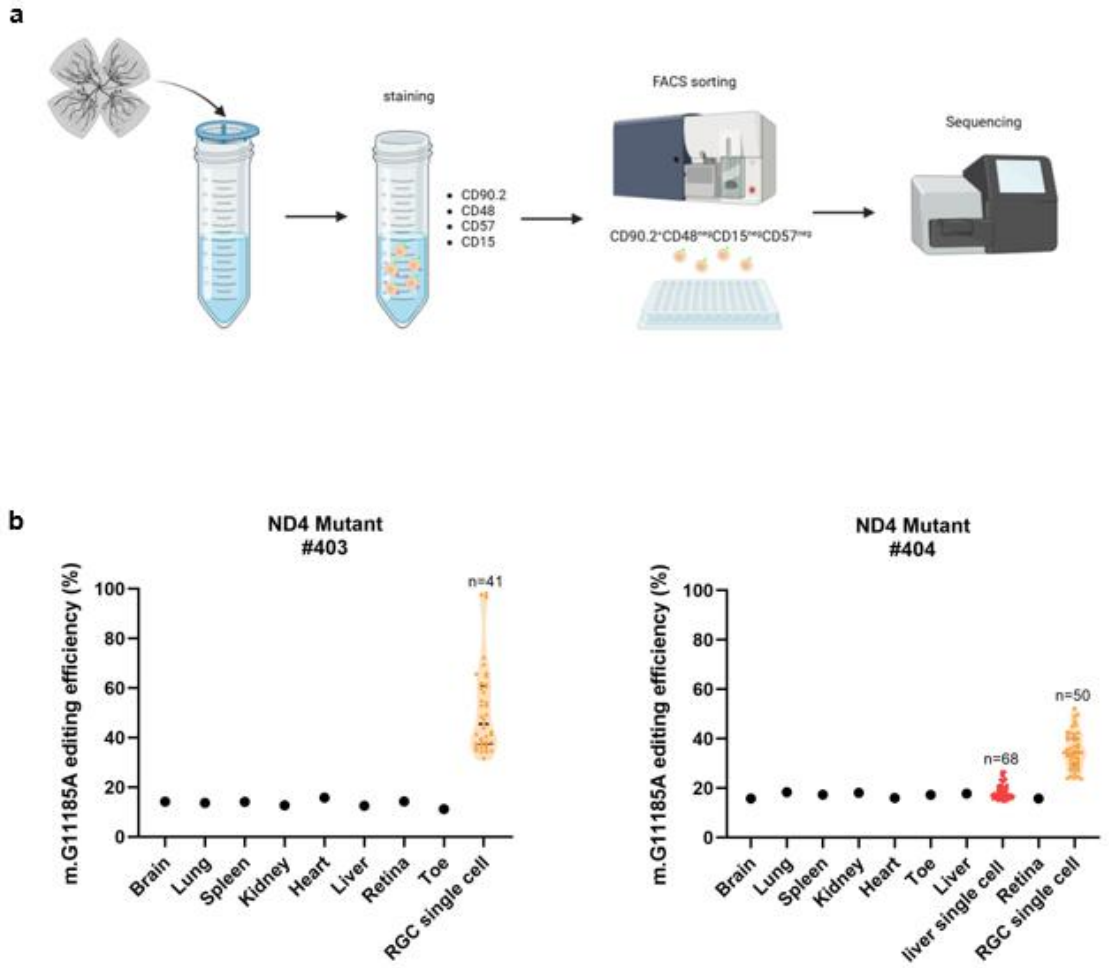

Supplementary Figure 8

Supplementary Figure 8. Genotyping results of retinal ganglion cells and tissues in *MT-MD4* mutant mice.

a. Schematic illustration of methods for isolating retinal ganglion cells in mouse retina. Created in BioRender. Kim, K. (2025) https://BioRender.com/q83ja0f

b. Editing efficiencies in m.G11185A locus from *MT-ND4* mutant mice tissue and retinal ganglion cells (RGC). Each red dot indicates single liver cells, and each orange dot indicates single RGCs. The number of cells were represented on top of plot. Thick bar indicates median, and thin bars indicate quartile value.

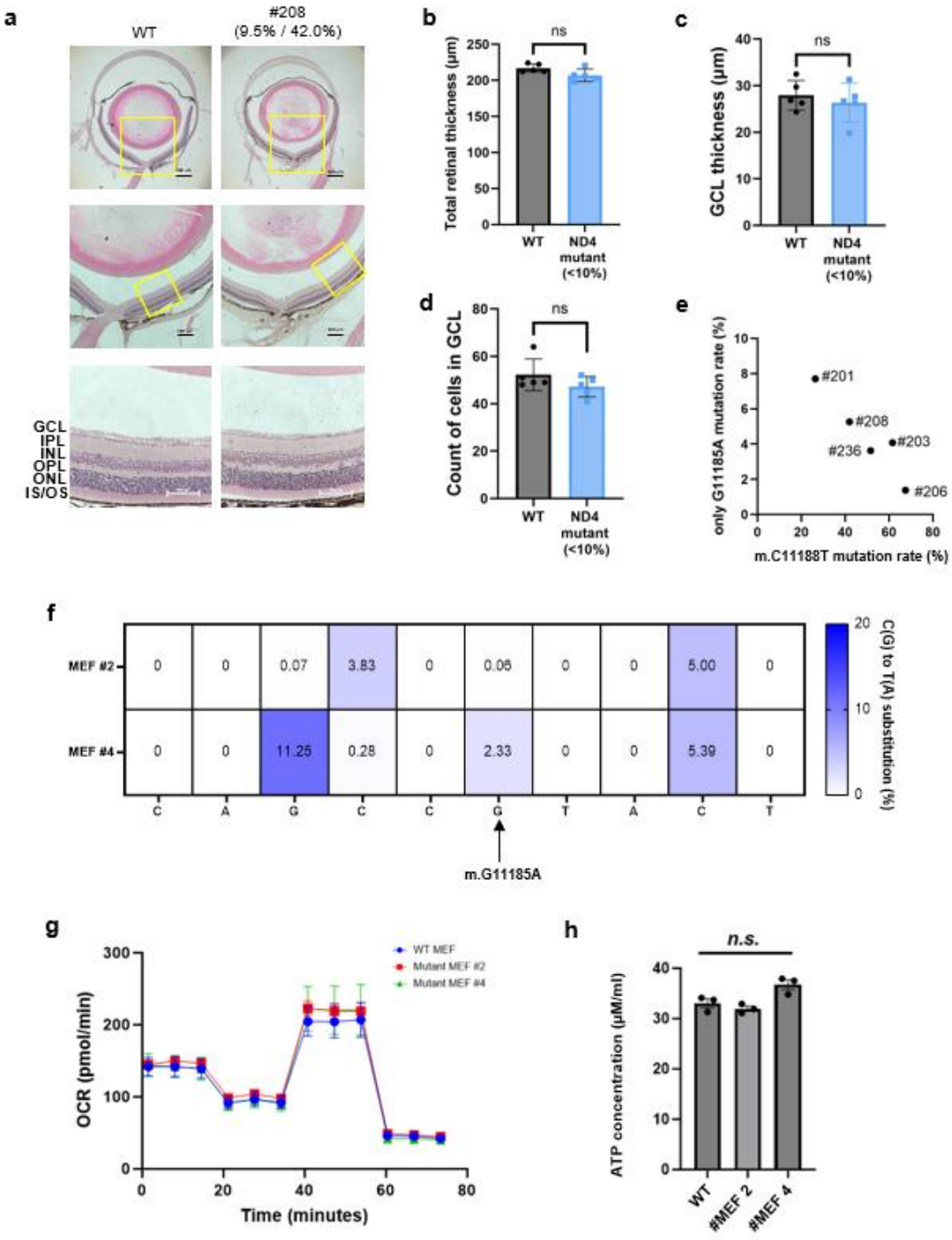

Supplementary Figure 9

Supplementary Figure 9. Histological and mitochondrial functional analysis of mutant mice and MEF cell line with higher m.G11182A and m.C11188T editing efficiency.

a. Histological analysis of eyeball sections stained with H&E in WT, and *MT-ND4* mutant mice with m.G11185A heteroplasmy levels below 10% and m.G11182A and m.C11188T editing efficiency above 20%. Enlarged parts indicated magnifications of the yellow boxed area in upper to rows, and magnifications were 4x, 10x, 40x in each.

b. Analysis of retinal thickness in WT, and *MT-ND4* mutant mice with m.G11185A heteroplasmy levels below 10% and m.G11182A and m.C11188T editing efficiency above 20%. The exact p-values for *MT-ND4* mutant mice compared with WT mice was 0.07. Error bars indicate s.e.m. for biologically independent mice (n=5) (ns, not significant using Student's two-tailed t-test).

c. Analysis of GCL thickness with m.G11185A heteroplasmy levels below 10% and m.G11182A and m.C11188T editing efficiency above 20%. The exact p-values for *MT-ND4* mutant mice compared with WT mice was 0.5. Error bars indicate s.e.m. for biologically independent mice (n=5) (ns, not significant using Student's two-tailed t-test).

d. Analysis of cell counts in GCL with m.G11185A heteroplasmy levels below 10% and m.G11182A and m.C11188T editing efficiency above 20%. The exact p-values for *MT-ND4* mutant mice compared with WT mice was 0.2. Error bars indicate s.e.m. for biologically independent mice (n=5) (ns, not significant using Student's two-tailed t-test).

e. Genotyping results for *MT-ND4* mutant mice used in histological analysis.

f. A heatmap showing base substitution in *MT-ND4* mutant MEF cell line #2 and #4.

g. Oxygen consumption rates of mouse embryonic fibroblasts. Each respiratory parameter was normalized to the value of the WT. For #MEF 2, and #MEF 4, the m.G11185A editing efficiencies were 0.06% and 2.33%, respectively. The error bars indicate the s.e.m. for replicates (n=4).

h. ATP concentrations in the MEF cell lines of WT and *ND4* mutant. The error bars indicate the s.e.m. for biologically independent samples (n=3). (ns, not significant using Student's two-tailed t-test)

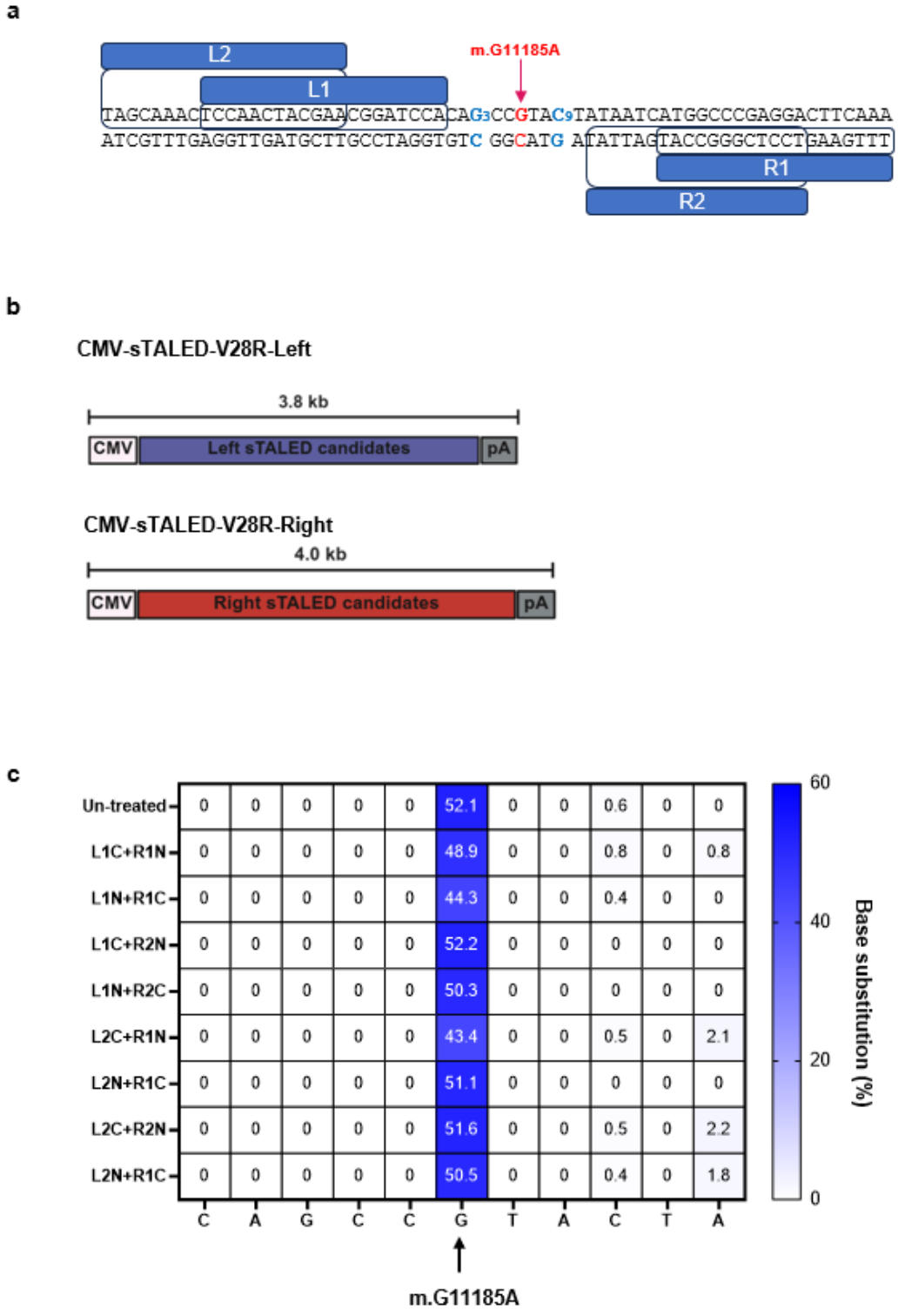

Supplementary Figure 10

Supplementary Figure 10. Genotyping results for screening sTALED-V28R candidates for mitochondrial gene therapy.

a. TALE combinations for (m. G11185A) targeted sTALED-V28R candidates. TALE sequences were numbered with white letters and indicated by navy boxes. Desired editing locus are shown in red (m. G11185A), and probable undesired edits were shown in blue (m.G11182A and m.C11188T).

b. Schematic construct of sTALED-V28R plasmids.

c. A heatmap showing base substitution in *MT-ND4* mutant MEF cell line #6 after treating sTALED-V28R plasmid via lipofection. Each TALE combinations were indicated on y axis, and desired editing window were represented on x axis. The on-target (m.G11185A) locus represented with arrow. Data were shown as means from n=3 biologically independent samples.

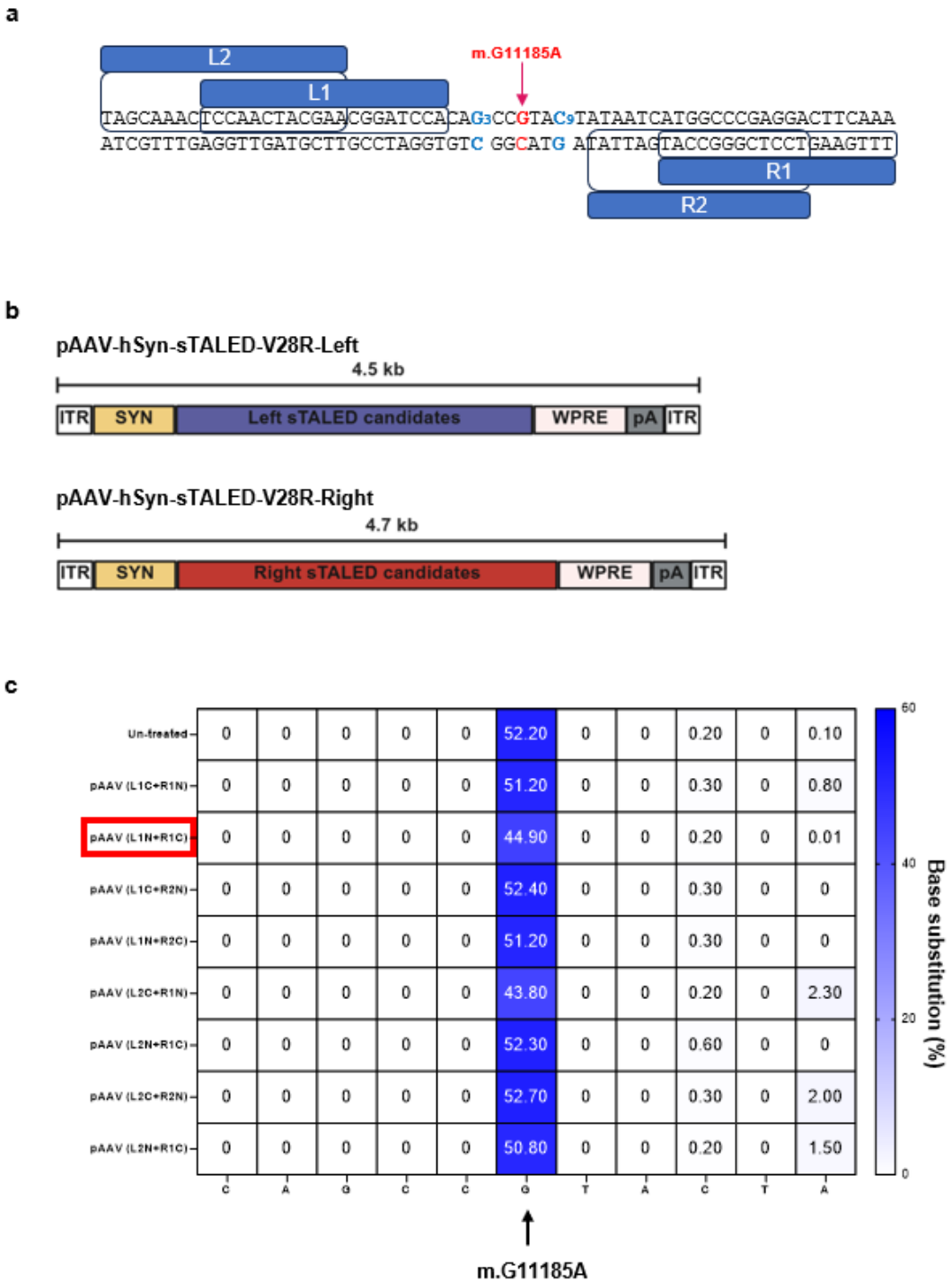

Supplementary Figure 11

Supplementary Figure 11. Genotyping results for screening sTALED-V28R-AAV candidates for mitochondrial gene therapy.

a. TALE combinations for (m. G11185A) targeted sTALED-V28R-AAV candidates. TALE sequences were numbered with white letters and indicated by navy boxes. Desired editing locus was shown in red (m. G11185A), and probable undesired edits were shown in blue (m.G11182A and m.C11188T).

b. Schematic construct of sTALED-V28R-AAV plasmids.

c. A heatmap showing base substitution in *MT-ND4* mutant MEF cell line #6 after treating sTALED-V28R-AAV plasmid via lipofection. Each TALE combinations were indicated on y axis, and desired editing window were represented on x axis. Selected final candidate was shown in the red box. The on-target (m.G11185A) locus represented with arrow. Data were shown as means from n=3 biologically independent samples.

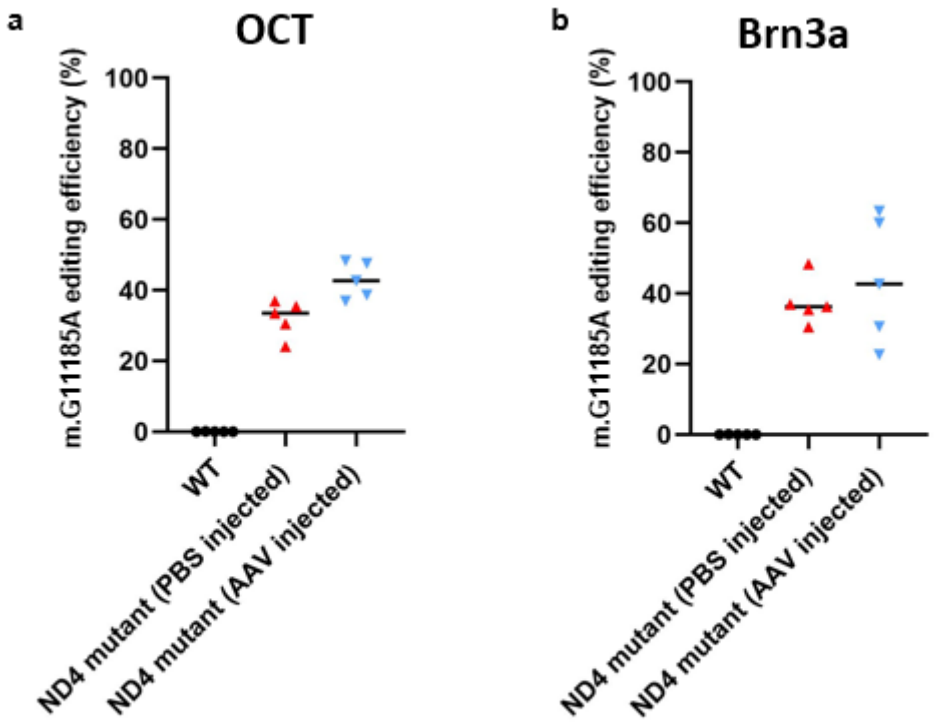

Supplementary Figure 12

Supplementary Figure 12. Genotyping results of *MT-ND4* mutant mice used in histological and OCT analysis. 5.

a. Genotyping results of *ND4* mutant related to Fig. 5. Each dot blots mean individual mutant mice. Each dot blot indicates individual mice. Bar indicates median value.

b. Genotyping results of *ND4* mutant related to Fig. 5. Each dot blot indicates individual mice. Bar indicates median value.

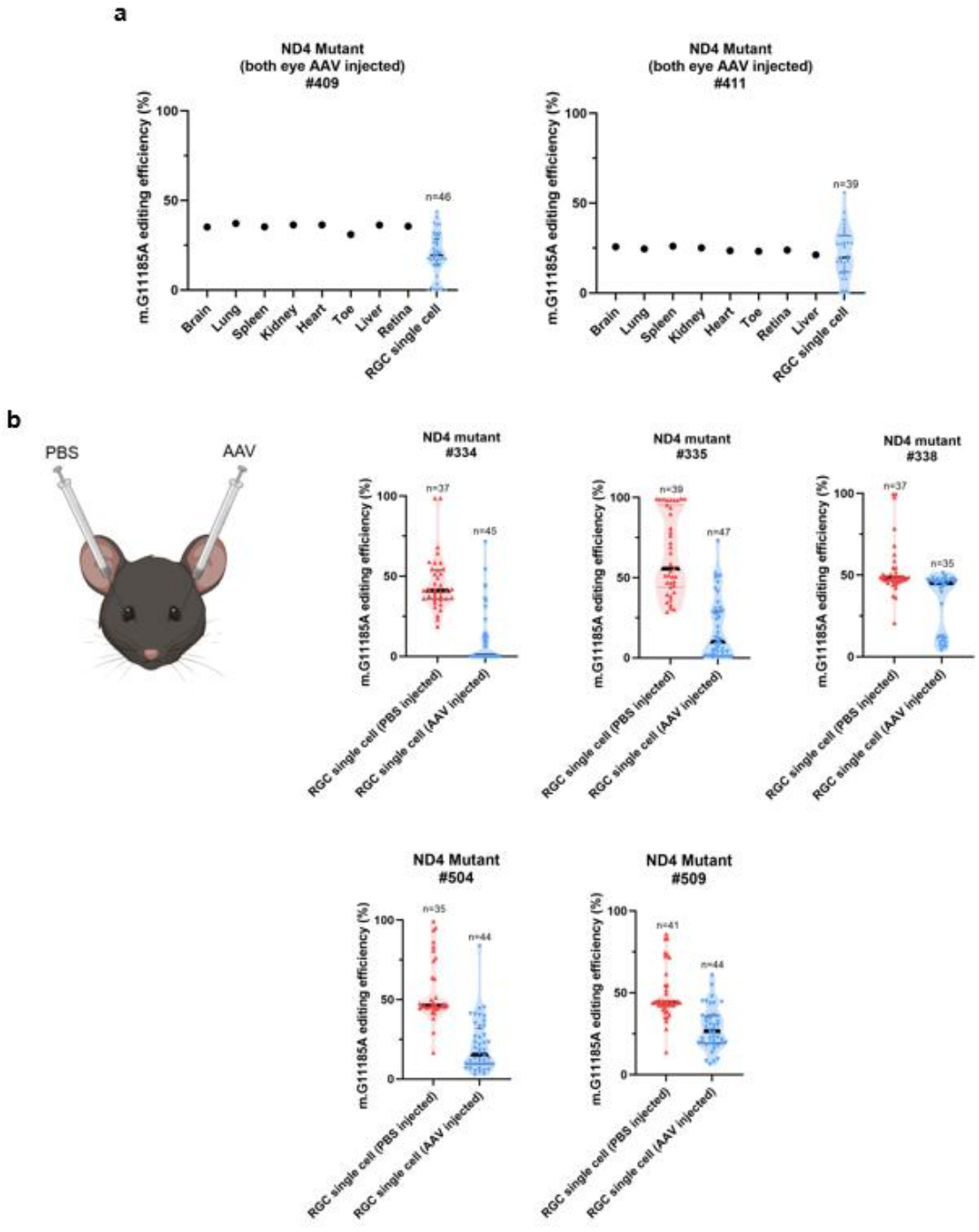

Supplementary Figure 13

Supplementary Figure 13. Genotyping results of retinal ganglion cells and tissues in sTALED-V28R-AAV injected *MT-MD4* mutant mice.

a. Editing efficiencies in m.G11185A locus from *MT-ND4* mutant mice tissue and retinal ganglion cells (RGC). Both eyes were intravitreally injected with AAV. The number of RGCs used in genotyping were indicated with bold on top of plot. Thick bar indicates median, and thin bars indicate quartile value.

b. Schematic illustration showing intravitreal injection of PBS and AAV into eyes of *ND4* mutant mice. Editing efficiencies in m.G11185A locus from *MT-ND4* mutant mice tissue and retinal ganglion cells (RGC). RGCs with PBS injected were shown in red dots, and AAV-injected RGCs were shown in cyan dots. The number of RGCs used in genotyping were indicated with bold on top of plot. Thick bar indicates median, and thin bars indicate quartile value. Created in BioRender. Kim, K. (2025) https://BioRender.com/5idozma

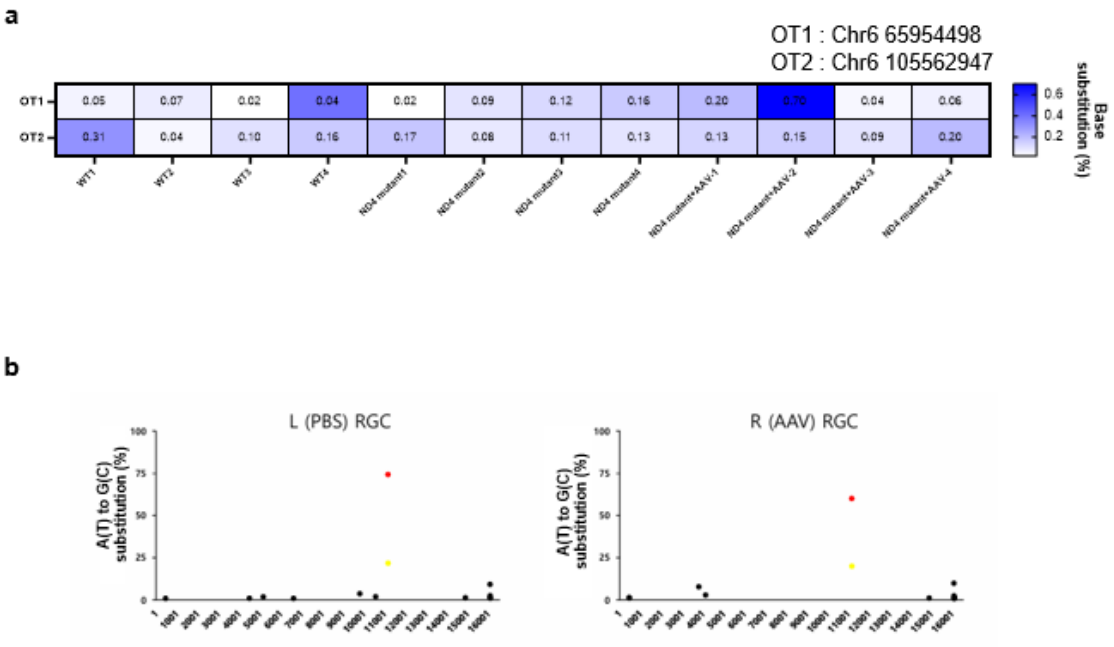

Supplementary Figure 14

Supplementary Figure 14. Off-target genotyping results of *MT-ND4* mutant mice.

a. Nuclear off-target analysis with WT, *ND4* mutant, and AAV-injected *ND4* mutant mice. Off-target sites were selected by under 2 nucleotide mismatches. Data were shown as means from n=3 replicates.

b. Base substitution in whole mitochondrial genome of RGC from AAV-injected ND4 mutant mice. On-target (m.G11185) efficiencies were shown in red, and undesired edits were shown in yellow (m.G11182A and m.C11188T).

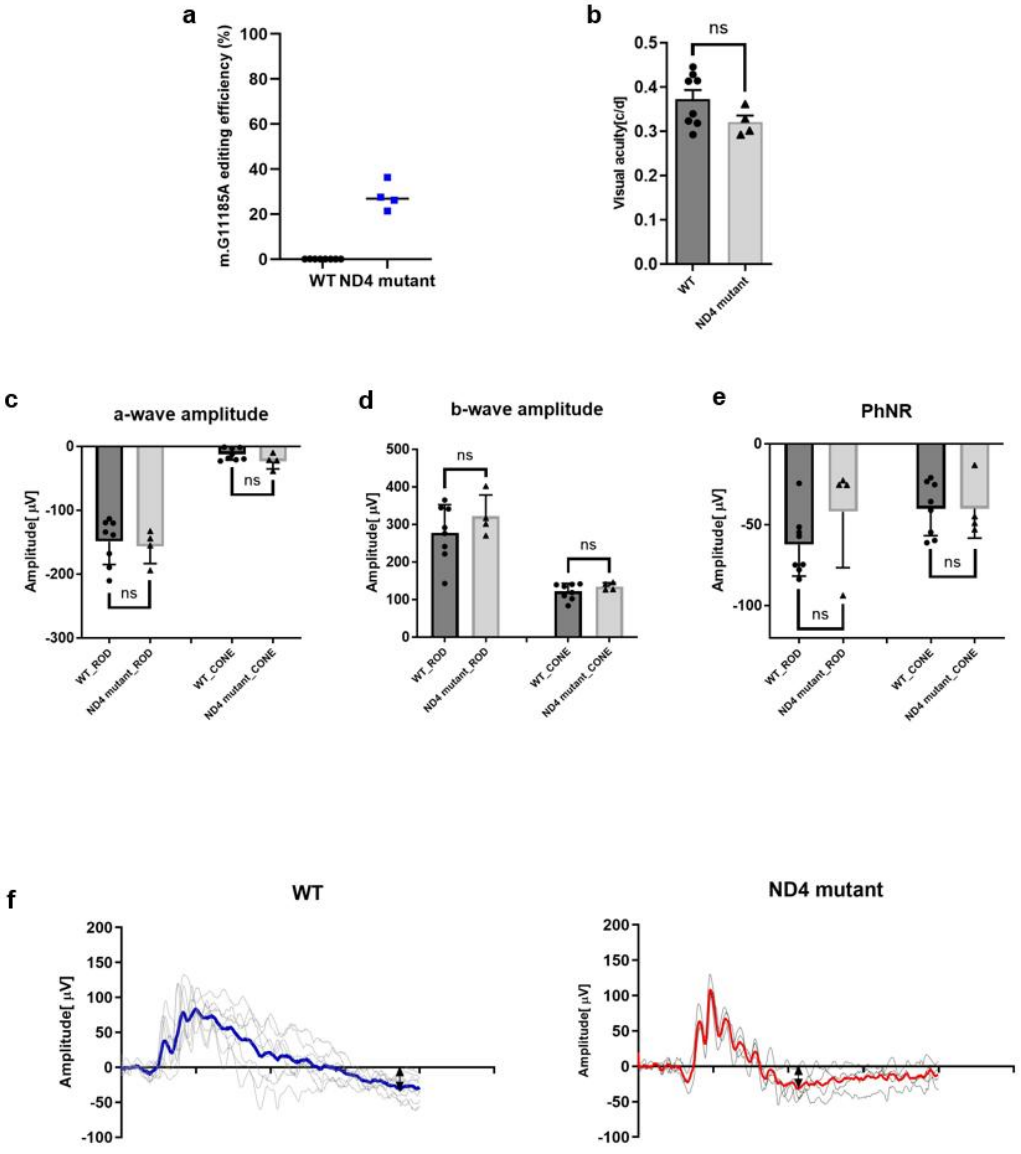

Supplementary Figure 15

Supplementary Figure 15. Visual function analysis of *MT-ND4* Mutant Mice using OKN and ERG.

a. m.G11185A editing efficiency in 17-week-old mice with visual phenotypes, with independent samples for each group (WT, n=8; *MT-ND4* mutant, n=4). Bar indicate median value.

b. visual acuity measured in 17-week-old WT, and *MT-ND4* mutant mice, showing no significant difference between the two groups. Error bars indicate standard error of the mean (s.e.m.) for biologically independent mice (ns, not significant using Student's two-tailed t-test).

c. a-wave amplitude measured in 17-week-old WT, and *MT-ND4* mutant mice, showing no significant difference between the two groups. Error bars indicate standard error of the mean (s.e.m.) for biologically independent mice (ns, not significant using Student's two-tailed t-test).

d. b-wave amplitude measured in 17-week-old WT, and *MT-ND4* mutant mice, showing no significant difference between the two groups. Error bars indicate standard error of the mean (s.e.m.) for biologically independent mice (ns, not significant using Student's two-tailed t-test).

e. Photopic negative response (PhNR) measured in 17-week-old WT, and *MT-ND4* mutant mice, showing no significant difference between the two groups. Error bars indicate standard error of the mean (s.e.m.) for biologically independent mice (ns, not significant using Student's two-tailed t-test).

f. Recorded electronic waves used in ERG analysis of WT and *MT-ND4* mutant mice. Individual mouse waves are shown in gray, and the average wave for each group is shown as a bold line. Arrowheads indicate the PhNR (photopic negative response) peak.

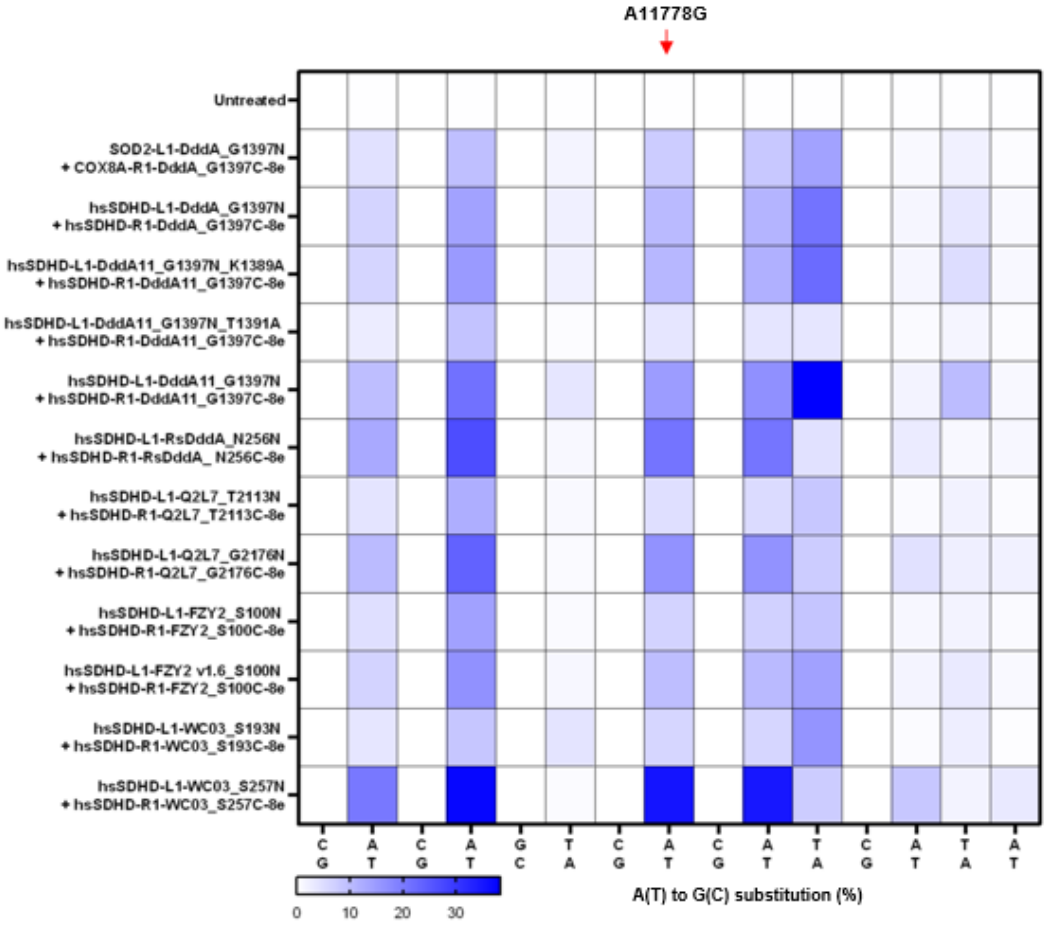

Supplementary Figure 16

Supplementary Figure 16. WC03 DddA homolog applying sTALED (esTALED) increases on-target editing efficiency and editing patterns are refined.

Heat map depicting A-to-G conversions caused by applying variable DddA variants and homologs to sTALED. Untreated sample was used as negative control. Data were shown as means from n=3 biologically independent samples.

a

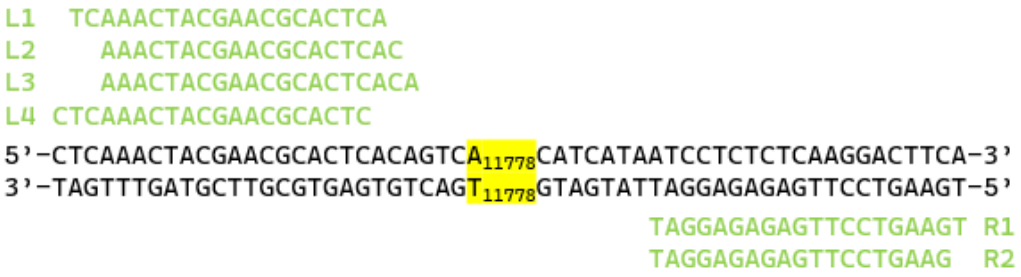

b

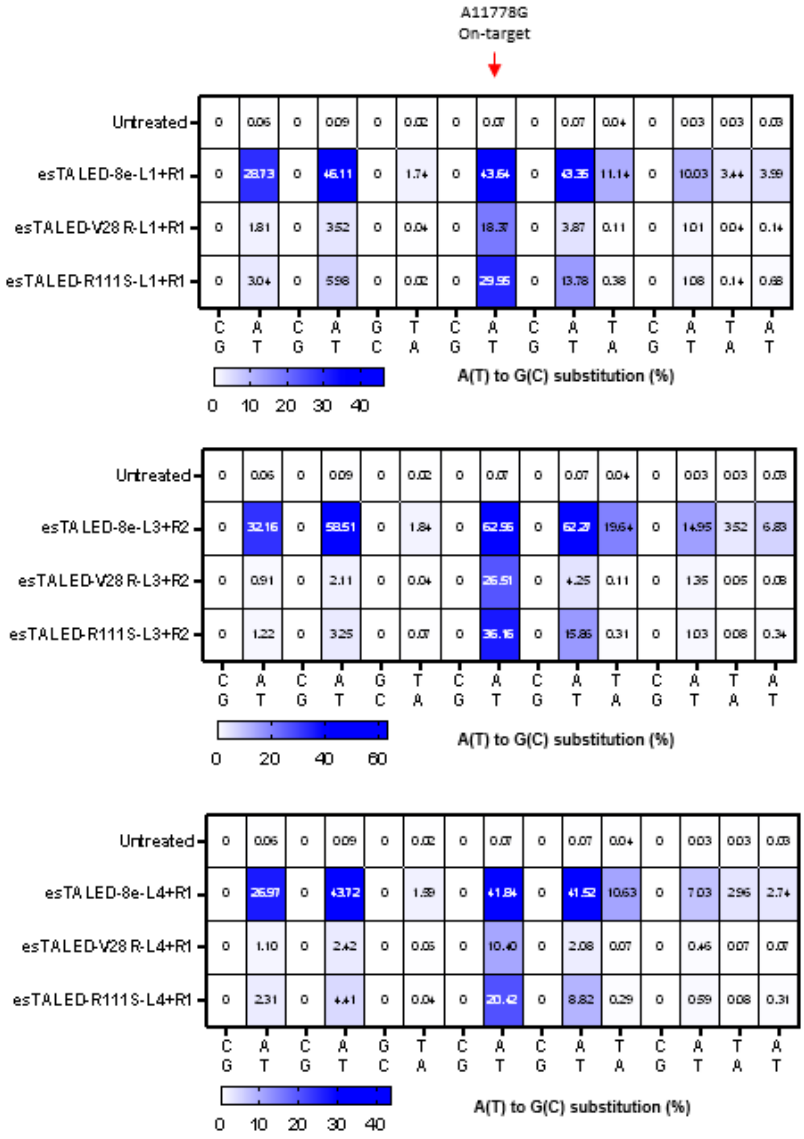

Supplementary Figure 17

Supplementary Figure 17. Optimization of editing window according to TALE binding location.

a. Architecture of different TALE binding sTALED pairs designed to target the m. G11778A in human *MT-ND4* gene. Double strand DNA sequence is near the *MT-ND4* m. G11778A mutation (yellow) that includes the TALE binding sequence for 4 left TALEs (L1, L2, L3, L4) and 2 right TALEs (R1, R2) are indicated.

b. Heat map depicting A-to-G conversions induced by combinations of different TALE binding locations each of esTALED-8e, esTALED-V28R TadA8e variant, and esTALED-R111S TadA8e variant. Untreated sample was used as negative control. Data were shown as means from n=3 biologically independent samples.

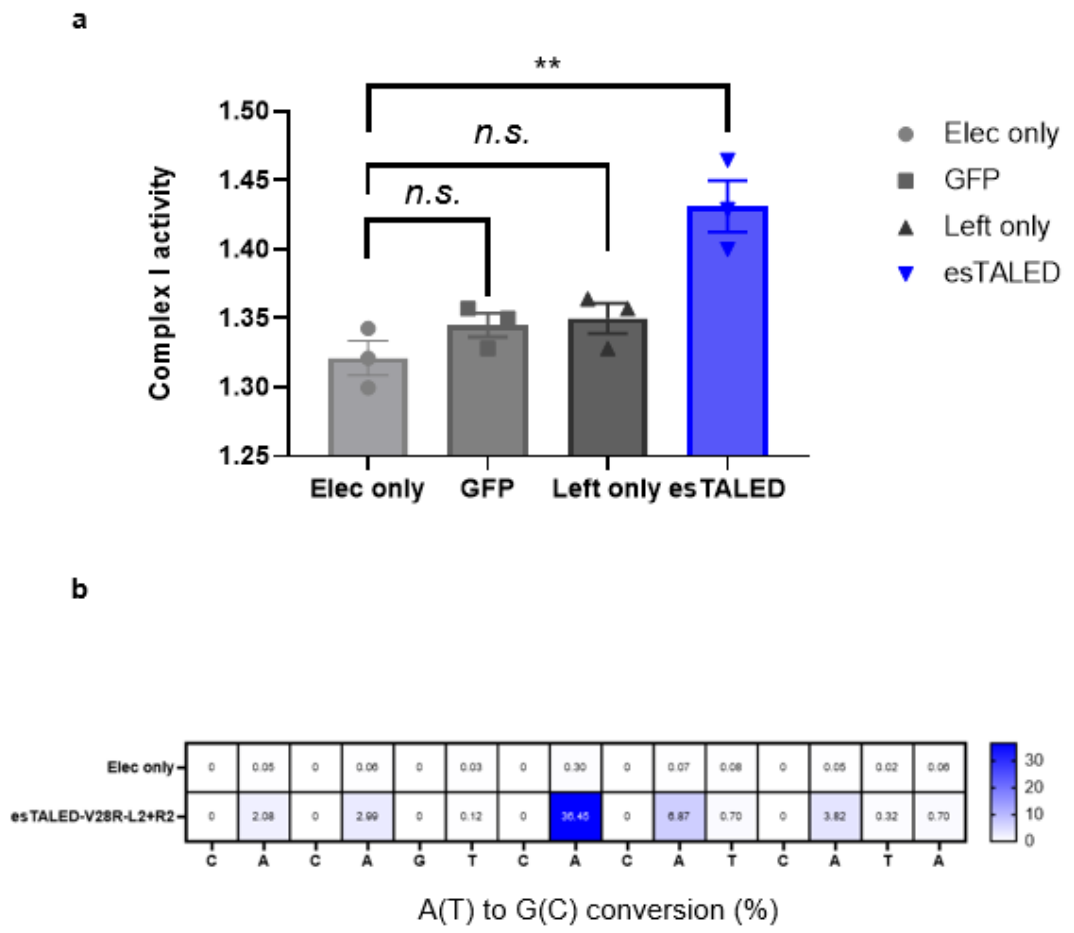

Supplementary Figure 18

Supplementary Figure 18. Mitochondrial complex I activity analysis of patient UDC.

a. Complex I activities in patient-derived UDCs. Electroporation only, GFP, Left-esTALED treated cells were used for negative control. Error bars indicate standard error of the mean (s.e.m.) for replicates (n=3). The exact p-values were 0.008 in Elec only and esTALED, 0.189 in Elec only and GFP, 0.158 in Elec only and Left only. (**p<0.01, ns, not significant using Student's two-tailed t-test).

b. A heatmap showing base substitution in electroporation only, esTALED-V28R-L2+R2 treated UDCs.

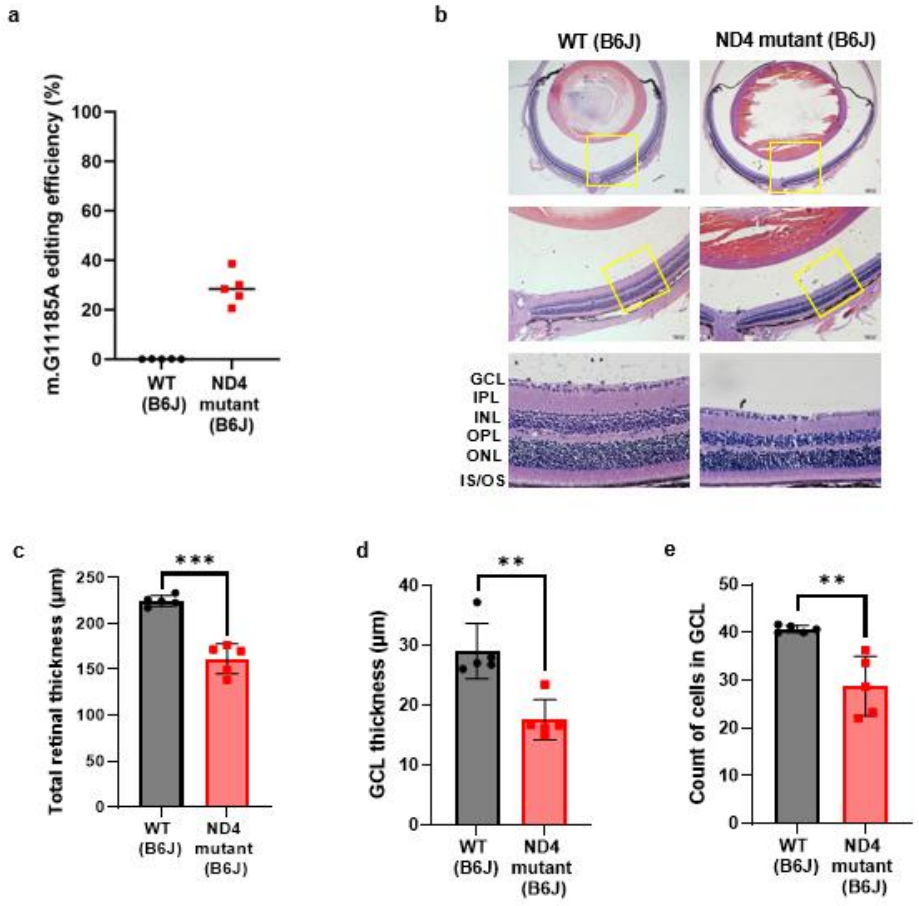

Supplementary Figure 19

Supplementary Figure 19. Histological anaylsis of WT and *MT-ND4* mutant mice from C57BL/6J strain.

a. Genotyping results for *ND4* mutant mice used in histological analysis.

b. H&E-stained retinal sections of WT and MT-ND4 mutant (n=5) mice. Enlarged views (4×, 10×, 40×) highlight layer alterations (GCL: ganglion cell layer, IPL: Inner plexiform layer, INL: inner nuclear layer, OPL: outer plexiform layer, ONL: outer nuclear layer, IS/OS: inner segment/outer segment).

c. Quantifications of total retinal thickness. Error bars indicate standard error mean (s.e.m.). Exact p value is 0.000038

d. Quantifications of GCL thickness. Error bars indicate standard error mean (s.e.m.). Exact p value is 0.0020

e. Quantifications of GCL cell counts. Error bars indicate standard error mean (s.e.m.). Exact p value is 0.0029.

Supplementary Tables

Supplementary Table 1. Number of mutant embryo and pups

Type of mutagenesis	Number of examined Embryos	Number of cultured 2-cell Embryos	Number of Blastocysts (%)	Number of transferred 2-cell Embryos	Number of Offspring (%)	Number of edited/total Blastocysts (%)	Number of edited/total Offspring
N/A (buffer injection)	20	20	15 (75)	NA	NA	0 (0)	NA
ND4 G11185A (DddA11 injection)	289	58	40 (69)	173	38 (21)	20 (50)	1 (0.03)
ND4 G11185A (Hifi-DdCBE injection)	82	20	16 (80)	58	8 (14)	15 (94)	8 (100)

Supplementary Table 1

Supplementary Table 2. Primers used in this study

Name	Sequence	Note
mMT-ND4 1st PCR F	CCTTCATCCTTCTCTCCCTAT	mtDNA NGS
mMT-ND4 1st PCR R	CGCGTTGGGTGGTAATAAT	mtDNA NGS
mMT-ND1 1st PCR F	TGTTCCCAGAGGTTCAAATC	mtDNA NGS
mMT-ND1 1st PCR F	GAAATTGTTTGGGCTACGG	mtDNA NGS
mMT-ND4 2nd PCR F	ACACTCTTTCCCTACACGACGCTCTTCCGA TCTCAGTTAGCCACATAGCACTT	mtDNA NGS
mMT-ND4 2nd PCR R	GTGACTGGAGTTCAGACGTGTGCTCTTCCG ATCTGTGGCTATAAGTGGGAAGAC	mtDNA NGS
mMT-ND1 2nd PCR F	ACACTCTTTCCCTACACGACGCTCTT CCGATCTTCGCCATAGCCTTCCTAA	mtDNA NGS
mMT-ND1 2nd PCR F	GTGACTGGAGTTCAGACGTGTGCTCTT CCGATCT GTGTGAGTGATAGGGTAGGT	mtDNA NGS
hMT-m.G11778A 1st PCR F	TACGGACTCCACTTATGACTCC	mtDNA NGS
hMT-m.G11778A 1st PCR R	GGGTGAGTGAGCCCCATTG	mtDNA NGS
hMT-m.G11778A 2nd PCR R	ACACTCTTTCCCTACACGACGCTCTTCCGA TCTCCCTCGTAGTAACAGCCATTC	mtDNA NGS
hMT-m.G11778A 2nd PCR R	GTGACTGGAGTTCAGACGTGTGCTCTT CCGATCTTAAGGCGAGGTTAGCGAGG	mtDNA NGS
mtWGS-1 F	TCTCCGTGCTACCTAAACACC	mtDNA WGS
mtWGS-1 R	GGCTGAGGTGAGGATAAGCA	mtDNA WGS
mtWGS-2 F	GTACGATGGCCAGGAGGATA	mtDNA WGS
mtWGS-2 R	CTTCCCACTGTACACCACCA	mtDNA WGS